Circular dichroism of distorted double gyroid thin film metamaterials

Emily K. McGuinness, Benjamin R. Magruder, Kevin D. Dorfman, Christopher J. Ellison, and Vivian E. Ferry *Department of Chemical Engineering and Materials Science, University of Minnesota, 421 Washington Avenue SE, Minneapolis, Minnesota 55455, USA

(Received 20 June 2024; revised 7 October 2024; accepted 30 October 2024; published 20 November 2024)

Strong circular dichroism (CD) has been reported in triply periodic, co-continuous gyroid thin films for certain orientations and surface terminations. However, processing of gyroid thin films introduces distortions experimentally, creating a mismatch between the structures created practically and those explored computationally. This work explores the impact of compression normal to the substrate (z-compression) with conserved volume in (110)-oriented plasmonic silver double gyroid thin films on CD using finite-difference time-domain (FDTD) simulations. As compression reaches 15% and above, new features emerge including termination-dependent opposite-handed CD responses and, at larger compressions, shorter wavelength responses that span many surface terminations. The longest wavelength responses of the system redshift with increasing compression. The top surface structure contributes strongly to the emerging opposite-handed features and redshifting of wavelengths. However, the less surface termination-dependent features arise from a mixture of contributions from the top surface and interior of the films. Interplay of these leads to CD-switching phenomena as a function of compression for certain terminations and wavelengths. When alternative methods are utilized to compress the system, such as compression with a Poisson's ratio of 0.33 (comparable to polystyrene) or the generation of compressed equilibrium structures with nonaffine strut changes via self-consistent field theory, similar optical responses persist. Overall, this study highlights the significant impact experimentally relevant distortions (especially compression and some nonaffine structural shifts) can have on the CD response of block copolymer templated plasmonic double gyroid thin films, and it provides mechanistic insight into the film interior versus surface contributions to the CD response during compression.

DOI: 10.1103/PhysRevMaterials.8.115201

I. INTRODUCTION

Circular dichroism (CD), the differential absorption of left and right circularly polarized light, is of interest for applications including anticounterfeiting and security structures [1], miniature photonics components [2], molecular chirality sensing [3], and protein structure characterization [3]. These applications either necessitate or benefit significantly from a strong CD response. The strength of a CD response can be quantified by the numerical difference in absorption of left versus right circularly polarized light as well as by the g-factor (Kuhn's dissymmetry factor) which normalizes CD to the average absorption at a particular wavelength. Optical metamaterials created from inherently chiral nanostructures generally lead to an orders of magnitude stronger CD response than their molecular counterparts [2].

Block copolymer self-assembly, a bottom-up approach, creates periodic structures of the requisite feature size for CD responses at visible and near-infrared wavelengths [4–7]. Driven by a competition between interfacial tension and minimizing polymer chain stretching, block copolymers self-assemble into a variety of morphologies depending upon the relative volume fraction of each polymer block. For a diblock copolymer, one morphology of interest is the double

*Contact author: veferry@umn.edu

gyroid, which is comprised of two interpenetrating, opposite-handed, triply periodic single gyroid networks of one block in a matrix of the other with overall cubic symmetry $Ia\bar{3}d$. Each component single gyroid network of the double gyroid structure possesses chiral geometric elements, such as helices and screw axes [8,9]. In certain orientations of these dielectric single gyroid structures, photonic band gaps from Bloch modes couple with a significant circular dichroism index to yield a CD response [10,11]. The optical responses can be tuned across different wavelengths of light by engineering the lattice parameter of block copolymer structures (from roughly 30 to 100 nm) via selection of the polymer chemistry, molecular weight of the block copolymer, and polymer architecture [12].

While the structures created directly from block copolymer self-assembly can offer the requisite chirality for the system, the resulting structures are dielectric materials with a relatively low refractive index and lattice parameters too small to support a significant CD response. To provide reasonable functionality for optical metamaterial applications, the introduction of an inorganic component (for example, a high refractive index dielectric material or a plasmonic metal) into one polymeric domain is often employed [7,13]. By selectively substituting one domain of the gyroid structure with a plasmonic metal (gold, silver, aluminum, etc.), plasmonic resonances can also be introduced yielding complex responses with additional design considerations [5,8,14,15].

Double gyroid structures were long anticipated to have minimal CD response, as the double gyroid structure is composed of two opposite handed single gyroid networks, rendering it achiral. However, most double gyroid-forming materials that have been studied for optical applications are processed into thin films with distinct and relatively uniform surface structures where the unit cell terminates. Recent computational studies have demonstrated the dominating influence of surface termination in nanoscale plasmonic gyroid thin films on both linear dichroism and CD response (g-factors as high as 0.25) [5,15]. The CD response of (110)-oriented double gyroid thin films in particular varies significantly with the surface structure, which depends upon the distance through the unit cell where the top plane of the structure exists [15]. As most applications for optical metamaterials from block copolymers involve creating thin films rather than bulk structures, this surface effect is both a highly relevant and enabling feature for engineering CD responses.

With each processing step used to create and template selfassembled structures in thin films, distortions to the double gyroid unit cell are introduced that have not been previously considered for their impact on CD response. In the simplest case, where films are spin cast and then thermally annealed to reach their equilibrium gyroid morphology, there is slight compression normal to the film surface [16]. When alternative approaches such as solvent vapor annealing (SVA) are used to access the gyroid morphology, even larger distortions arise including both compression and nonaffine gyroid strut modifications (local strut thinning, thickening, or relative shifting in position) [16-19]. Due to compression of oriented films normal to the substrate, distortions usually shift the film from cubic symmetry to triclinic symmetry. For example, poly(2hydroxyethyl methacrylate)-block-poly(methyl methacrylate) double gyroid thin films contracted normal to the substrate by 45% from the swollen state to the dry state during solvent vapor annealing in a mixed vapor environment [17]. Templating self-assembled thin films with inorganic structures is a further source of distortions such as compression and nonaffine changes [20,21]. For example, sol-gel processing to create silica gyroid structures leads to film shrinkage by roughly 7.5% of their original thickness [20]. Distortions even exist in systems that could be considered to be bulk, with slice and view SEM revealing local symmetry breaking via the nonaffine variation of gyroid strut lengths and diameters (although the angular geometry remains near constant) [22]. While a variety of distortions can exist across experimental systems, compression normal to the substrate in thin films is largely unavoidable and a predominant mechanism of distortion.

The impact of these common distortions on the CD response of nanoscale gyroid films is largely unexplored. In this work, we systematically evaluate via finite-difference time-domain (FDTD) simulations the influence of compression normal to the substrate in plasmonic templated gyroid thin films with structural parameters derived from experimental work. While theoretical analysis of periodic dielectric network structures such as gyroids has been demonstrated in the literature [10,11], the additional plasmonic nature of the structures in this work (which closely matches materials used to evoke CD in experiments) makes analytical analysis unfeasible. Therefore, finite-difference time-domain simulations

to numerically solve Maxwell's equations are required. To understand the role of compression alone, distortions in this work are first considered to be uniform and follow strict volume conservation, resulting in orthorhombic unit cells, and they do not include nonaffine changes in the relative gyroid strut dimensions. These affine compressions introduce new features to the CD spectra including short-wavelength CD responses that are surface-termination-independent, redshifting of long-wavelength responses, and opposite handed CD responses. As certain features arise and intensify with compression, a CD switching behavior results, highlighting the potential to use compression as a means for CD response control. Affine compression results are then compared with compression including nonuniform changes in gyroid struts by using thermodynamically equilibrated structures from polymer self-consistent field theory (SCFT) as input for FDTD simulations. SCFT is a state-of-the-art technique for calculating the equilibrium morphology and free energy of block polymer phases [23]. Previous work has combined simulations of Maxwell's equations with SCFT derived block copolymer structures to compute photonic band gaps of dielectric materials [24]. In a similar manner, the SCFT to FDTD pipeline described in this work provides an understanding of increasingly realistic block copolymer-based network structures while expanding the capabilities of the optical simulations to include additional phenomena (CD) and materials (plasmonic metals). The nonaffine compressions explored demonstrate a similar appearance of new CD features as a function of compression, but generally exhibit stronger CD.

II. METHODS

A. Finite-difference time-domain simulations

Following methodologies and formalisms similar to those described by Cote *et al.*, to compute CD spectra of the structures in this work, finite-difference time-domain simulations were run under left and right circularly polarized light (LCP and RCP) illumination (injected from the positive *z* to the negative *z* direction). Monitors were used to capture both reflected and transmitted radiation. As the sum of transmission, reflection, and absorption is unity for these systems, absorbance can then be directly computed. The difference in absorption under left versus right circularly polarized light is then plotted as CD spectra [15]. An example of this process is shown in Fig. S1 [31]. Note that the wavelength of an absorption maximum is not necessarily the same as peaks in CD response.

The gyroid structures themselves all originated from self-consistent field theory simulations (see Sec. IIB). These structures were converted to .stl filetypes via MATLAB code and then imported into commercial FDTD software (Ansys Lumerical). The morphology, volume fraction, orientation, and nonaffine distortions were controlled via SCFT while the amount of uniform compression was adjusted. The simulated structures were modeled as silver gyroid networks with an air matrix. The refractive index of silver was modeled via a Lorentz-Drude Debye fit to complex refractive index data from Palik [25].

Absorbed optical power for the spatial absorption studies was computed through Eq. (1) from the permittivity (ε) and

the electric field intensity (E) at the wavelength of interest (in angular frequency ω),

$$P_{\rm abs} = -0.5\omega |E|^2 \text{Im}(\varepsilon). \tag{1}$$

B. Self-consistent field theory

Self-consistent field theory calculations were performed using the open-source PSCF software [26–28], which solves the standard SCFT equations in a periodic unit cell, representing the polymer chain using the continuous Gaussian chain model [23]. The relevant equations and numerical methods implemented in PSCF have been described in detail elsewhere [26].

To calculate the equilibrium structure for the double-gyroid morphology when compressed along the [110] direction, we began by obtaining an uncompressed SCFT solution in the conventional cubic unit cell for the $Ia\bar{3}d$ space group. The lattice parameter a was allowed to relax to an optimum value in this calculation. For a block volume fraction of 0.52 and $\chi_N = 20$, this value was 4.27 $N^{1/2}b$, where chi is the Flory-Huggins parameter, N is the total degree of polymerization, and b is the statistical segment length for both the A and B blocks (which we set to be equal to one another for simplicity). We then rotated this solution into a new orthorhombic unit cell in which the lattice basis vector **c** points along the [110] direction. Finally, we incrementally changed the lattice parameters of this orthorhombic unit cell, solving the SCFT equations in a rigid unit cell at each step using the solution from the previous step as an initial guess. In this process, we reduced the value of c while increasing a and b such that the volume of the unit cell is conserved and the ratio a:b was kept constant. We obtained 24% compression along [110] before subsequent calculations no longer converged.

III. RESULTS AND DISCUSSION

To explore the influence of compression on an experimentally relevant system, plasmonic silver double gyroid structures (as have been templated in the literature from block copolymers via electrodeposition [7]) with an air matrix were evaluated using finite-difference time-domain (FDTD) simulations. The simulated volume fraction of silver (0.52) and lattice parameter (51.7 nm, $4.27N^{1/2}b$) were based on experimental double gyroid thin films created via the thermal annealing of asymmetrically disperse polystyreneblock-poly(D,L)lactide (PS-b-PLA) [29]. This study primarily explores the (110) double gyroid orientation, which has been observed experimentally in thin films [5,16] and has previously demonstrated both a strong circular dichroism (CD) and linear dichroism response [5,15]. Throughout this work, x, y, and z Cartesian axes are assigned to point along the [001], [110], and [110] directions and will be referred to accordingly. Light is injected from the positive z direction to the negative z direction. The film thickness in this work is eight d-spacings (planar periodicities) thick, which, in the (110), is approximately 292.5 nm ($d_{110} = 36.6$ nm). Lattice parameter, volume fraction, material, refractive index of the matrix, thickness, defect density, and surface termination have all been previously explored for plasmonic gyroid forming materials, therefore these parameters are kept constant

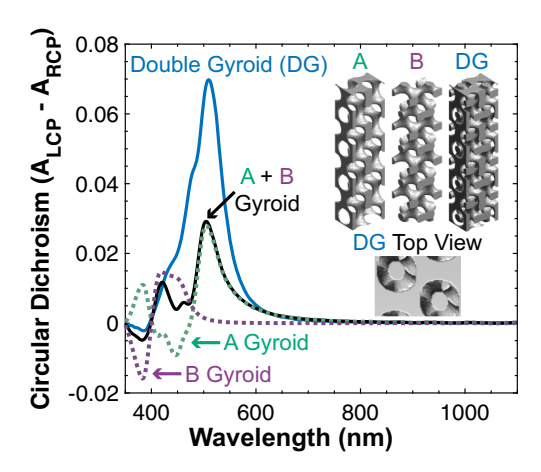


FIG. 1. Finite-difference time-domain (FDTD) simulated circular dichroism spectra for (440)-terminated plasmonic silver gyroid network structures with an air matrix including a 0.52 volume fraction double gyroid (blue solid line), the "A" single gyroid network with a volume fraction of 0.26 (green dotted line), and the "B" single gyroid network of the same volume fraction (purple dotted line), as well as the sum of the circular dichroism of the "A" and "B" structures (black solid line) in thin films (\sim 292 nm thick). Inset are three-dimensional illustrations of the single and double gyroid networks as modeled, as well as a top view of the double gyroid structure with internal struts that are visible in the subsurface.

unless germane to understanding the impact of compression on CD response [5,15]. For this work, the surface structures are assumed to be free of additional distortions that may arise due to exposure to a surface (free or substrate) despite these likely occurring in thin film systems [30].

The double gyroid structure is a bicontinuous network comprised of two intertwining, opposite handed single-gyroid networks (illustrated individually as "A" and "B" in Fig. 1). In the double gyroid morphology, the two networks are the same chemical composition (here silver) within a matrix of different chemical composition (here air, removed for illustration). Within the (110)-oriented plasmonic double gyroid structure, these two single gyroid networks are offset from each other by half a d-spacing vertically. Due to this offset, the surface of a (110)-oriented double gyroid thin film exhibits patterns that are not composed of opposite equivalent structural components [unlike several other orientations, such as the (211)]. Throughout the film interior, the offset between the single gyroid networks creates a pattern that is not opposite equivalent at any horizontal plane through its depth.

The simulated CD spectra of the two-component single gyroid networks alone (green and purple dotted lines), their simple addition (solid black), and the (440)-terminated double gyroid structure (solid blue) are shown in Fig. 1. Consistent with prior literature reports [5,15], the single gyroid networks exhibit nearly opposite equivalent bisignate CD responses at short wavelengths, while at longer wavelengths, the (440)-terminated "A" gyroid network exhibits a CD response that is not mirrored in the spectra of the "B" gyroid network. The switching of handedness around a central wavelength (the Cotton effect) is known to arise when the handedness of incident circularly polarized light matches the handedness

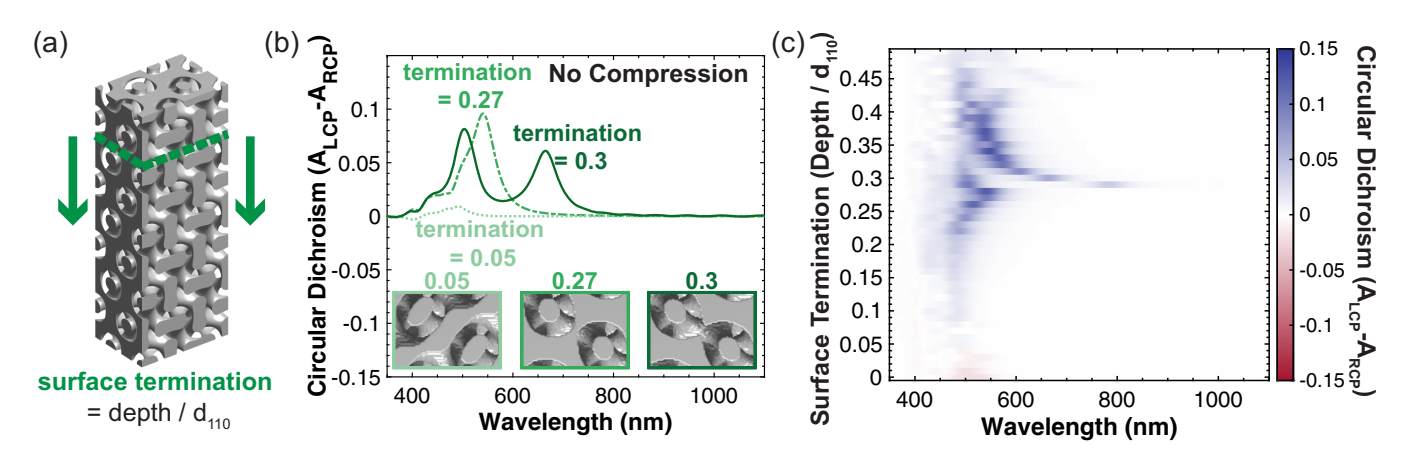


FIG. 2. (a) Illustration of slicing through a double gyroid structure to reveal different surface terminations, reported as the slice depth normalized to the d-spacing of the (110) orientation. (b) FDTD simulated circular dichroism spectra for silver double gyroid structures with an air matrix for surface terminations of 0.05 (light green, dotted line), 0.27 (green, dashed line), and 0.3 (dark green, solid line). Top-down views of the double gyroid structure are inset for each termination. (c) Simulated circular dichroism spectra illustrated as heatmaps, blue being left circularly polarized (LCP) light absorption dominant, and red being right circularly polarized (RCP) light absorption dominant, as a function of surface termination (y-axis).

of a plasmonic helical structure, pointing towards a possible subsurface mechanism for the shorter wavelength responses [2]. The longer wavelength CD response of the "A" gyroid network, on the other hand, is likely surface structure dominated as explored in prior studies [5,15]. The CD response of the equivalent surface structure of the "B" gyroid network (found half a *d*-spacing away) exactly mirrors that of the "A" gyroid network.

As a result of their offset in the [110] direction, the simple addition of the two single gyroid network's CD spectra is nonzero despite the opposite handed symmetry. Consistent with prior literature, the double gyroid structure's CD response is even stronger than that of the simple addition of the single gyroid network components and features additional peaks, indicating the two plasmonic networks are coupled [15]. In fact, despite overall higher absorption (Fig. S2) [31], the double gyroid thin film modeled here has a maximum *g*-factor of 0.098 which is almost twice that of the maximum *g*-factor for the "A" single gyroid network (0.047). Orientations of double gyroid structures that do not possess this offset of single gyroid networks, such as the (211), exhibit minimal CD response (Fig. S3) [15,31].

As prior literature simulations have used slightly different volume fractions and lattice parameters [15], the surface structure-dependent response is shown for this system in Fig. 2. Figure 2(a) illustrates and defines surface termination as the distance from the (110) plane (or depth) normalized to the d-spacing (or interplanar spacing) of the (110). In this definition, the previously discussed (440) termination has a surface termination value of 0.25. To maintain thickness, the quantity removed from the surface is replaced on the bottom of the film. In this way, the top and bottom surfaces of the structure are symmetric for all simulations.

Figure 2(b) shows CD spectra for three different (110) plasmonic film terminations with top views of the double gyroid structures (matrix removed) inset. Consistent with prior findings [5,15], the CD spectra vary significantly with the surface termination for both large structural differences

such as those between 0.05 and 0.27 and smaller structural changes such as the breaking of connectivity along the surface structures. To demonstrate this influence systematically across surface terminations, Fig. 2(c) condenses each CD spectra into a heatmap with dark blue representing a CD of 0.15, white representing a CD of 0, and dark red representing -0.15 (with the gradient corresponding accordingly). Positive values (blue) indicate left circularly polarized (LCP) light preferential absorption, while negative values (red) correspond to right circularly polarized (RCP) light preferential absorption. Simulations are only conducted to 0.49 because after this point the response is opposite, but equivalent as a result of the space-group symmetry of the double-gyroid morphology (Fig. S4) [31]. The general behavior of the surface termination-dependent CD response corresponds well to that of prior studies which used a smaller volume fraction and larger lattice parameter [15]. However the quantitative responses are not equivalent, highlighting the role of gyroid structure fill fraction in CD response.

To investigate how the CD response of plasmonic double gyroid thin films changes with compression, thin films [structure illustrated in Fig. 3(a)] were systematically compressed from 2% to 45% in the z-direction (normal to a hypothetical substrate). The compression was performed by changing the lattice parameters of the structure in a manner that conserved total unit-cell volume. As a result, when the surface normal direction was compressed by 45%, the lateral directions expanded by roughly 35%. As surface termination significantly impacts the CD response, all terminations in the system were considered for each compression. Figures 3(b)–3(f) show the surface termination-dependent CD response (as heatmaps) for 5%, 15%, 25%, 35%, and 45% z-compression with volume conserved. Figure S5 shows the equivalent plots for 2%, 7%, 10%, 20%, 30%, and 40% compression [31].

When (110) silver double gyroid structures are compressed, CD responses for all surface terminations undergo overall modest changes through 10% z-compression, indicating relative stability of the response to minor compression.

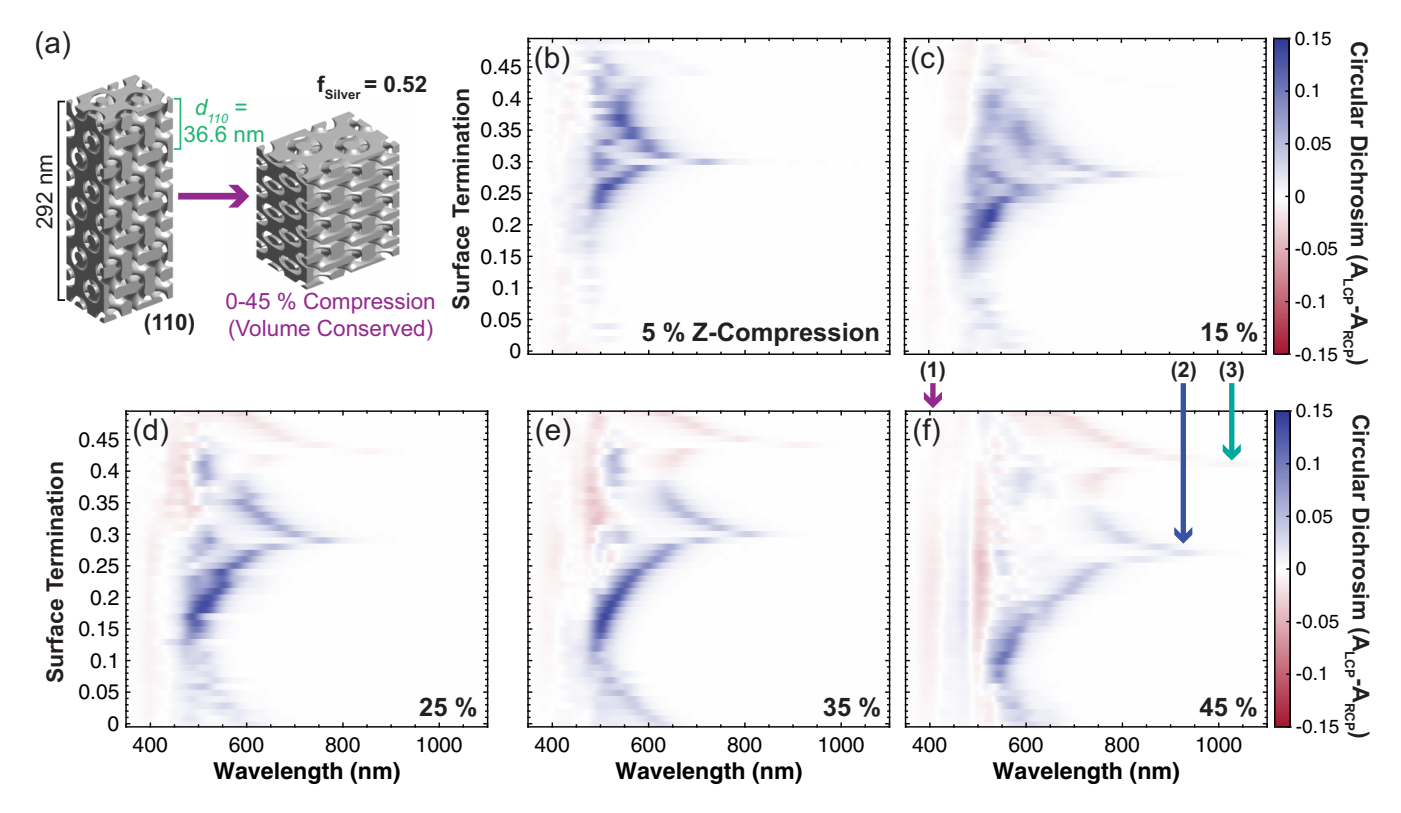


FIG. 3. (a) Illustration of plasmonic silver double gyroid thin films modeled here and key parameters for study. Heatmaps of surface termination-dependent CD spectra for (b) 5%, (c) 15%, (d) 25%, (e) 35%, and (f) 45% percent z-compression (with volume conserved) of silver double gyroid thin films. Features of interest are labeled to facilitate discussion.

As compression increases to 15% and beyond, three main changes become clear: the emergence of CD responses that broadly span surface terminations at shorter wavelengths [an example of this is labeled as feature 1 with a purple arrow in Fig. 3(f)], the redshifting of the longest wavelength CD responses (feature 2, blue arrow), and the appearance of additional RCP light preferential absorption features (feature 3, green arrow). Consistent with uncompressed double gyroid thin films, the CD response at 45% compression is still equivalent, but opposite handed for surface terminations spanning 0.5–0.99 (Fig. S4) [31]. Figure S6 plots the *g*-factor and wavelength of the strongest and longest wavelength peak CD responses as a function of compression, which are also listed in Table SI [31].

Three CD responses emerge with compression that span multiple surface terminations: an RCP dominant response around 402 nm (feature 1), an LCP dominant response around 478 nm, and another RCP dominant response around 513 nm. To investigate whether these features mechanistically arise primarily from top surface or interior geometric elements, absorption of left and right circularly polarized light was evaluated spatially throughout the gyroid structure for select terminations and wavelengths. After integrating at each depth of the structure and taking the difference in absorption, Fig. 4 shows the cumulative CD as a function of depth [normalized to the d-spacing of (110)] for wavelengths and terminations that correspond to features labeled 1, 2, and 3 all at a compression of 45%. Additional cumulative absorption depth profiles are also provided in Figs. S7-S11. The multitermination response of feature 1 exhibits a slight initial LCP dominant response at its surface that diminishes and switches to an RCP dominant response after the first 36.6 nm (equivalent to one *d*-spacing of depth). After this point, the CD response oscillates with depth, ultimately maintaining an RCP dominant response.

Similar film interior driven CD responses are observed for the multitermination responses that emerge with compression at 478 and 513 nm. These responses are due to plasmonic coupling between the two gyroid networks (they are not observed

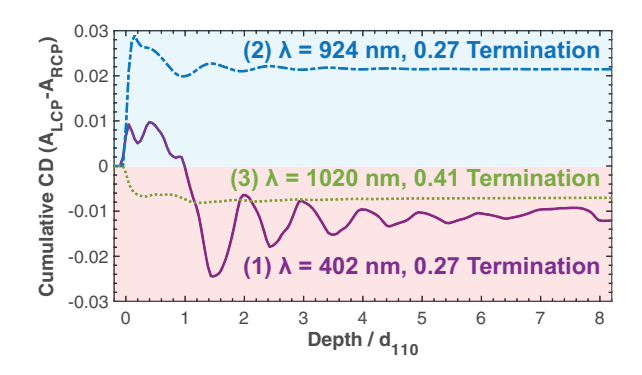


FIG. 4. Cumulative CD as a function of normalized depth for select responses under 45% compression including the multisurface termination RCP response at 402 nm and 0.27 surface termination (purple, solid), the longest wavelength LCP response at 924 nm and 0.27 surface termination (blue, dashed), and the longest wavelength RCP response at 1020 nm and 0.41 surface termination (green, dotted). All plots are for 45% *z*-compression (with volume conserved).

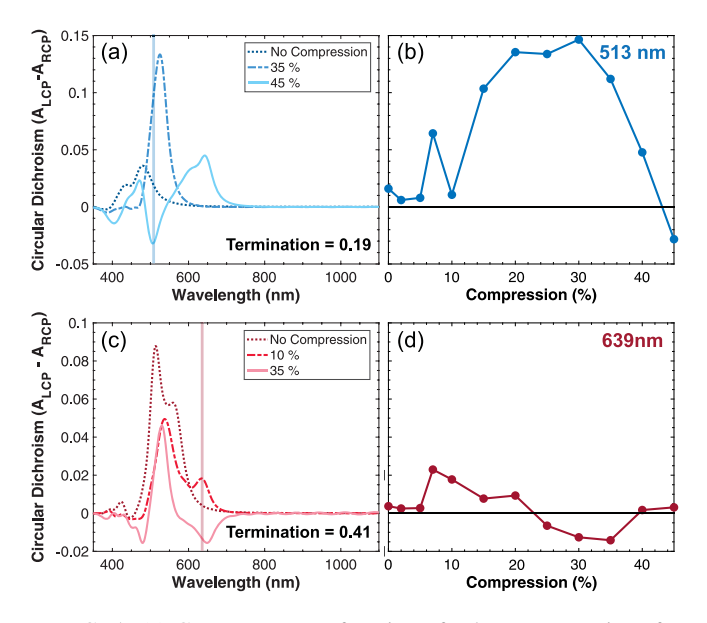


FIG. 5. (a) CD spectra as a function of select compressions for a termination of 0.19, and (b) the CD response for all compressions at a wavelength of 513 nm. (c) CD spectra as a function of select compressions for a termination of 0.41, and (d) the CD response for all compressions at wavelength 639 nm.

in compressed single gyroid structures, as shown in Fig. S12) and are not the result of an effectively larger unit cell in the lateral plane (Fig. S13, Table SII) [31]

The general redshifting of long-wavelength CD responses with compression (feature 2) is also explored in Fig. 4. For all considered compressions, the CD responses of this and similar features are found to be strongly surface-driven. However, the redshifting observed for the structure simulated with a larger lattice parameter (corresponding to 45% z-compression) is less than that observed in the compressed case, indicating that changes in the 2D projection of the surface alone are insufficient to explain these shifts (Fig. S13) [31].

The third feature of interest is the emerging RCP dominant response at longer wavelengths (feature 3), and its cumulative depth profile is plotted in Fig. 4. These responses appear at 15% compression and cannot be attributed to the size increases of the two-dimensional surface structure (Fig. S13) [31]. Much of the CD response for this feature is captured in the compression of one single gyroid network alone (Fig. S12), indicating that plasmonic coupling of this response is less dominant than in the shorter wavelength features [31].

The development of these new spectral features with compression introduces a CD switching phenomenon as a function of compression (for certain terminations and wavelengths). The full CD spectra for the double gyroid thin films with a surface termination of 0.19 at select compressions is shown in Fig. 5(a). Figure 5(b) examines the CD response of the double gyroid thin film under 513 nm illumination for all simulated compressions, revealing that the CD response as a function of compression strengthens from weakly LCP dominant when uncompressed to a stronger LCP dominant response through 30% compression before decreasing again in strength and ultimately switching to RCP dominant. Switching phenomena

that follow different patterns are observed for a number of terminations and wavelengths including 0.41 terminated double gyroid structures with representative full spectra shown in Fig. 5(c). Examining the CD response under 639 nm illumination reveals the CD response is originally minimal, becomes LCP dominated around 7% compression, switches to RCP dominant by 25% compression, and then returns to minimal [Figure 5(d)]. The origins of switching behavior are complex and vary with wavelength and termination. While the CD sign switching, for the conditions in Fig. 5(a), is not observed in the compression of the individual single gyroid networks or their simple addition, other conditions do show this correlation (Fig. S12) [31]. Overall, the observed switching may offer an opportunity to design systems with dynamic CD responses, which is of great interest for active metamaterials.

To explore the 513 nm CD switching response of the 0.19 terminated double gyroid thin film, the absorption of left and right circularly polarized light is once again computed spatially for the compressed double gyroid structures. Now, the contributions of each component single gyroid network to the overall absorption are also separated from within a single simulation. Figure 6 illustrates uncompressed, 25%, and 45% compressed 0.19 terminated double gyroid structures with "A" (green) and "B" (purple) gyroid network components color-coded. Plotted adjacently are LCP and RCP absorption as a function of depth (normalized to d_{110}) within each gyroid network and cumulative circular dichroism as a function of normalized depth. Due to the larger top surface contributions observed for certain structures, the top surface and film interior contributions are plotted on different scales in the absorption profiles.

Throughout the interior of all three gyroid films' structures, strong absorption of both LCP and RCP light occurs periodically as a function of the (110) gyroid structure's *d*-spacing. Reflective of the half *d*-spacing offset of the single gyroid networks, the "A" and "B" contributions alternate throughout the depth, with absorption from one generally peaking in the valley of the other. The absorption generally decreases in intensity as a function of depth as light attenuates, but there is stronger absorption at the back interface.

For the uncompressed double gyroid structure in Fig. 6(a), the top surface exhibits a relatively weak LCP dominant absorption, primarily driven by the "A" gyroid structure. The RCP and LCP absorption largely cancel throughout the film interior, resulting in a relatively weak final CD response that is similar to that observed in the first few nanometers. The 25% compressed double gyroid structure in Fig. 6(b) demonstrates significantly larger LCP absorption at the surface driven by the "A" gyroid network. However, the CD responses of the interior absorption are RCP dominated, leading to a gradual decrease in cumulative CD as a function of depth. The 45% compressed double gyroid thin film in Fig. 6(c) exhibits much weaker LCP surface absorption. As light travels below the surface, the response is complex with some points in the depth contributing towards an LCP response and others towards an RCP response. Eventually, the RCP dominated responses accumulate sufficiently to switch what was originally an LCP driven CD response to an RCP dominated one. Ultimately, as a function of compression, the 513 nm CD response of the 0.19 terminated double gyroid thin film switches

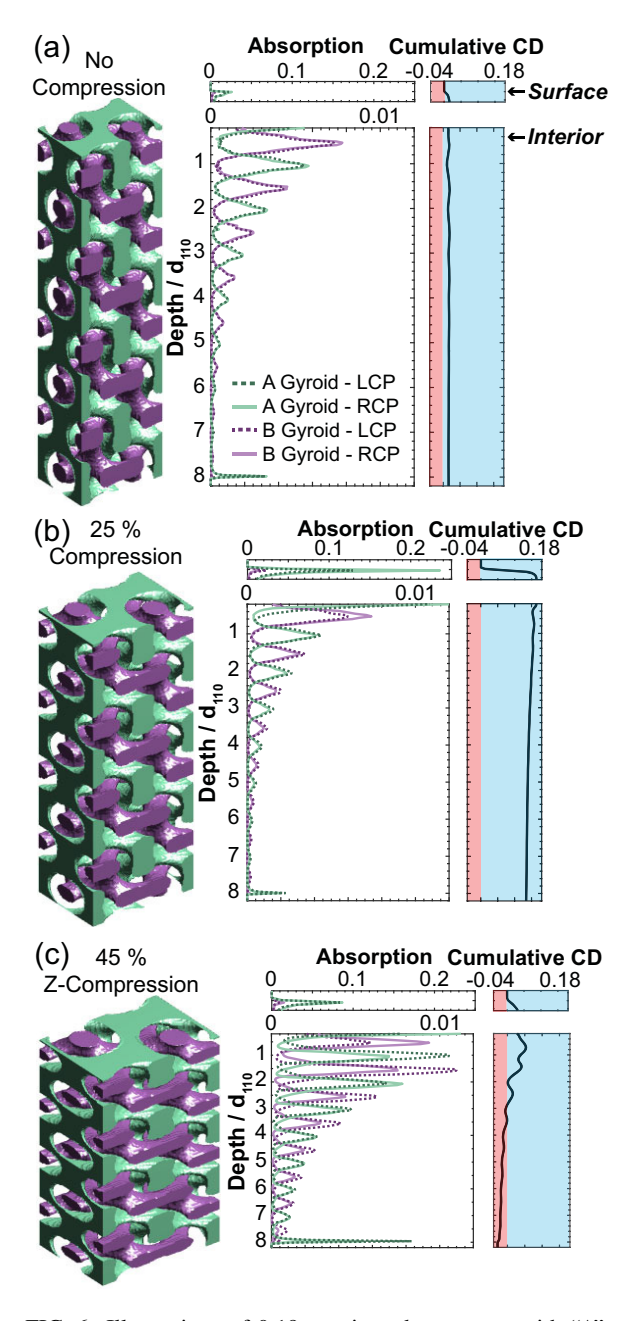


FIG. 6. Illustrations of 0.19 terminated structures with "A" and "B" single gyroid component networks selectively colored (green and purple, respectively) along with absorption of left and right circularly polarized light within each component single gyroid network under 513 nm illumination both at the surface (top) and throughout the film interior as a function of depth [normalized to the (110) *d*-spacing of the structure]. Also, cumulative circular dichroism as a function of normalized depth with blue highlighting left circularly polarized light dominated absorption and red highlighting right circularly polarized light dominated absorption. For (a) no compression, (b) 25% *z*-compression, and (c) 45% *z*-compression.

handedness because of a shift from a top surface to a film interior driven mechanism. In this case, the emergence of a film interior mechanism contradicts the surface, emphasizing the importance of purposeful engineering of film thickness, especially as compression occurs.

To better visualize the plasmonic contributions to the CD response as a function of compression, electric field enhancement spatial maps are examined in Fig. 7 for select regions of the data set corresponding to the results shown in Fig. 6. At the surface of the film all three compressions under these conditions exhibit an LCP dominant response. Figure 7(a) reveals that the enhancement of the electric field response occurs around the curved, narrow region of single gyroid network "A" as well as on the outer edges of the nanodots of single gyroid network "B." As z-compression is increased to 25%, the electric field enhancement of these locations strengthens and shows significant plasmonic coupling between the two single gyroid networks. However, as z-compression is further increased to 45%, the electric field enhancement again decreases, corresponding directly to the trends reported in Fig. 6. While generally similar in location, the electric field enhancement of the 25% z-compressed double gyroid thin film is distinctly different under left and right circularly polarized illumination, especially for the narrow region of the single gyroid network "A," likely accounting for the strong CD response observed at the surface of this particular structure. At roughly one d-spacing into the gyroid thin film's interior, there is little CD response for the uncompressed and 25% z-compressed films. However, the 45% z-compressed film exhibits an RCP dominant CD response at this depth. Examining the corresponding spatial electric field enhancement map reveals that the outer curvature of the gyroid network is a likely source of the differentiation in response to right and left circularly polarized light.

However, these structures are not two-dimensional in nature and are dictated by three-dimensional geometric elements rather than just planar ones. Figure 7(b) shows electric field enhancement spatial maps for unpolarized light (determined by adding the influences of right and left circularly polarized light) as a function of depth taken from slices across the diagonal of the XY plane [dashed lines in Fig. 7(a)]. The surface enhancement noted previously is shown to depend strongly on a thin semicircle slice of the "A" single gyroid network and its plasmonic coupling with the curvature of the underlying "B" single gyroid network with the strongest enhancement observed for 25% z-compression. Significant electric field enhancement is further observed throughout the depth of the 45% z-compressed double gyroid thin film in the air gaps between regions of curvature in the "A" and "B" single gyroid networks, again indicating strong plasmonic coupling under these conditions. Overall, these select observations point to changes in plasmonic geometries at the nanoscale as significant origins of the CD response of compressed double gyroids both at the surface and within the film interior. While correlating exact three-dimensional geometric contributions with the overall CD response is of great interest, it requires systematic examination of a larger data set and is beyond the scope of this work.

To generalize the observed compression induced CD responses across volume fractions, simulations were repeated at a volume fraction of 0.3 (Fig. S14) [31]. In the uncompressed state, the two volume fractions show qualitatively a similar surface structure-dependent LCP dominant CD response at long wavelengths. Slight differences include that the surface termination of the longest wavelength CD response is now

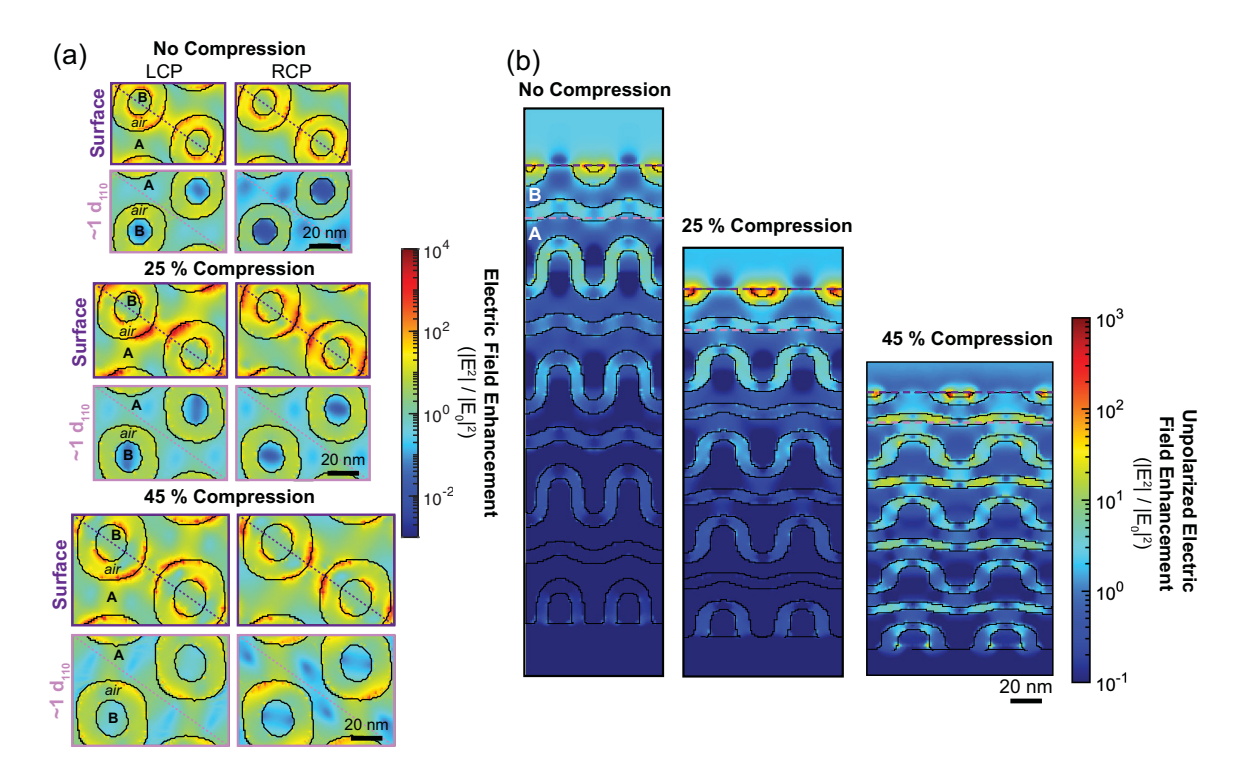


FIG. 7. (a) Spatial maps of electric field enhancement under left and right circularly polarized illumination for no compression, 25%, and 45% z-compression at the surface (dark purple outlines) and at one d-spacing of film depth (light purple outlines). The "A" and "B" component single gyroid networks of the silver structure as well as the air matrix are labeled accordingly. Colormaps are plotted on a logarithmic scale. (b) Unpolarized electric field enhancement spatial maps of the depth of the structure sliced along the diagonal [shown in (a)] for no compression, 25%, and 45% z-compression. "A" and "B" single gyroid component networks of the silver structure are labeled, and dotted lines indicating the surface and one d-spacing of film depth are included. Note the difference in color map scale range for the unpolarized electric field enhancement map. All maps are for the (110) silver double gyroid thin film with a surface termination of 0.19 under 513 nm illumination that is explored in Fig. 6.

at a termination of 0.2 rather than 0.29 and has a somewhat weaker overall response. Also, in contrast to the larger volume fraction, the smaller one exhibits an RCP dominant CD response across several terminations at a wavelength of about 500 nm with a maximum *g*-factor of 0.03 (Table SIII) [31]. Qualitatively, the observations made previously regarding the CD response of compressed (110) double gyroid thin films appear to translate across relevant volume fractions including the same three emergent feature categories. Interestingly, the emergent RCP dominant features are significantly stronger than those observed for the larger volume fraction case.

One limitation of this study is the use of volume conservation to remain tied to physical systems. To understand how different compression parameters may influence these results, simulations were also conducted using a Poisson's ratio of 0.333 (that of polystyrene) and compared with the volume conservation results (a Poisson's ratio of 0.5). The surface termination-dependent CD spectra of a 45% double gyroid structure compressed with a Poisson's ratio of 0.333 are shown in Fig. S15, and the maximum g-factor and longest wavelength are recorded in Table SIV [31]. Under this compression scenario, the lateral dimensions are about 10% smaller than in compression with volume conservation. The similarity of the results from the compression supports the previously noted lack of sensitivity to small symmetric stretching in the lateral structure.

Stretching in one lateral direction only, however, has a large impact on the CD response of the double gyroid structures. Applying volume conservation once more and stretching the structure in the y-direction by 5%, 10%, and 20% (which results in only 2%, 4%, and 9% compression), surface termination-dependent CD spectra were once more explored (Fig. S16) [31]. As a function of stretching, responses originally present, but subtle, in the unstretched case intensify significantly. For example, the maximum g-factor of the LCP dominant response increases substantially from 0.2 in the uncompressed case to 0.35 with 20% y-direction stretch (Table SV) [31]. In contrast to compression, these large changes in g-factor become significant with only mild degrees of stretching. Overall, the CD response following y-stretching is quite different from that of z-compression. Generally, if the gyroid structures were made from a flexible plasmonic material on a flexible substrate, these magnitudes of stretch may be readily accessible and provide additional access to dynamic or responsive devices.

Finally, in this study, all explorations of compression or stretching thus far have merely modified the lattice parameters of the gyroid unit cell and induced uniform changes in the gyroid struts. While these modifications give insight into the response of the gyroid structure under metastable processing and generally highlight compression as a tunable parameter, they may not be accurate in circumstances where the gyroid unit cell dynamically adapts to compression by

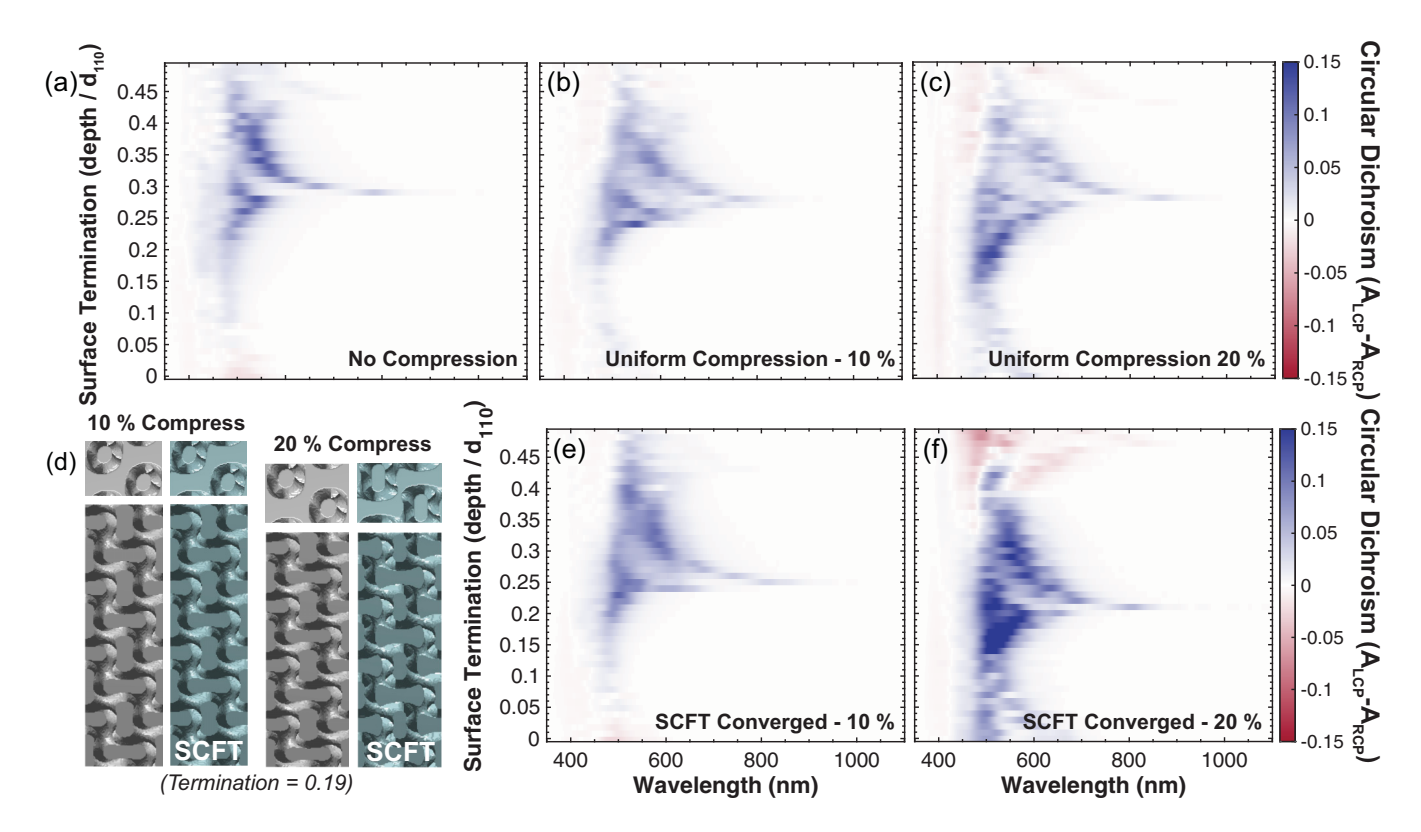


FIG. 8. (a) Surface termination-dependent CD spectra for the uncompressed double gyroid thin film (repeated for convenience) alongside the surface termination dependent CD heatmaps for (b) 10% and (c) 20% compressed (with volume conservation) double gyroid thin films via lattice parameter manipulation. (d) Illustration comparing uniformly compressed (gray) vs SCFT converged compressions (blue gray) at 10% and 20% compression (0.19 termination shown) along with surface termination-dependent CD spectra for the (e) 10% and (f) 20% SCFT compressed double gyroid structures. Note: Illustrated gyroid structures are different colors for visualization purposes only; silver was used to model all geometries.

modifying its local environment. Accessing physically informed nonaffine structural changes in gyroids and other network structures is challenging for optical modeling. To investigate how more complex, physically informed distortions impact the CD response, we developed a simulation pipeline leveraging polymer self-consistent field theory (SCFT) to generate compressed gyroid structures that were permitted to relax to their equilibrium configurations [26]. The lattice parameters for compression with volume conservation were set in the SCFT simulations, and an initial guess of a double gyroid thin film with a volume fraction of 0.52 was provided. The structures were then converged for each compression up to 24% (after which the simulations did not converge, indicating gyroid structures are unlikely to form at such extreme configurations under thermodynamic equilibrium). The output of these simulations was used as the input for FDTD simulations, demonstrating one of the first examples of this workflow. The surface termination-dependent CD responses for 10% and 20% uniform compressions versus SCFT converged gyroid structures are shown in Fig. 8 alongside illustrations of the structures. A summary table of largest g-factors and longest wavelengths is provided in Table SVI [31].

As seen in Fig. 8(d), the SCFT converged structures exhibit surface geometry variation alongside local thickening and thinning of gyroid struts (nonaffine changes). The surface

structure variations tend to occur in the connected regions of the surface structure which previously were demonstrated to have a strong impact on the CD response of the double gyroid thin films. The differences are significantly more pronounced for the 20% compressed structures than the structures with 10% compression. Overall, the CD spectra of the SCFT converged structures exhibit similar qualitative features including the appearance of long-wavelength RCP dominant features and weaker, but still present short wavelength multitermination responses. However, the magnitude of the CD response is significantly stronger for the SCFT converged structures than the uniformly compressed structures with the maximum LCP dominant response reaching a g-factor of 0.2 at 10% compression and 0.3 at 20% compression. The maximum RCP dominant CD also is intensified to 0.08 by 20% compression. These results highlight how the local geometry of the gyroid struts plays a significant role in the CD response of these metamaterials.

Capturing these distortions experimentally and accurately modeling them is an important area of continued research. Nonaffine distortions regularly occur due to thin-film confinement and general processing, such as those described for double-gyroid thin films in a recent SCFT study [30]. The nonaffine deformation example provided herein using SCFT as input for FDTD demonstrates how future studies can leverage the pipeline developed in this work for these

cases. Ultimately, this approach will be critical to better understanding the optical properties of these increasingly complex, physically informed structures.

IV. CONCLUSIONS

This work explores the influence of both uniform compression and compression that results in local structural changes on the circular dichroism response of silver double gyroid structures. The (110) orientation is explored due to the offset in component gyroid networks that permits a significant CD response in thin films, where surface structure plays a strong role. As the (110) double gyroid structure is compressed, the CD response changes with the addition of new features as well as shifts in CD intensity. Several features depend strongly on both the film surface and interior absorption of left and right circularly polarized light. The nature of the interior contributions varies throughout the depth of the structure, providing insight into engineering responses. Some CD responses switch as a function of compression, highlighting potential for the use of compression in dynamic devices. Further, these results translate across volume fractions and to some extent symmetric changes in the surface dimensions. Alternatively, stretching the double gyroid thin films in the y-direction contributes different types of responses with large g-factor increases as a function of stretching, again providing a pathway to dynamic systems. Finally, enabled by employing thermodynamically informed structures from SCFT in FDTD simulations, the impact of nonaffine changes in strut geometry

on CD response is explored. Overall, this work highlights the relevance of experimentally observed compressions and deformations to engineering the CD response of gyroid-derived 3D metamaterials thereby establishing an additional design parameter experimentally and intriguing opportunities for further mechanistic study of the origin of CD in 3D periodic, plasmonic metamaterials.

The data that support the findings of this study are available at the Data Repository for the University of Minnesota [32]. SCFT data presented in this work were generated using the open-source PSCF software, which is available at Github [33].

ACKNOWLEDGMENTS

The authors would like to sincerely thank Prof. Mahesh Mahanthappa, Prof. Michelle Calabrese, Dr. Jinwoo Oh, Dr. Szu-Ming Yang, Dr. Bryan Cote, Dr. Pengyu Chen, Dr. John Keil, and Maya Ramamurthy for instructive scientific conversations. This work was supported primarily by the National Science Foundation through the University of Minnesota MRSEC under Award No. DMR-2011401. E.K.M. was supported by the National Science Foundation through the eFellows Postdoctoral Fellowship program administered by the American Association of Engineering Education. The authors acknowledge the Minnesota Supercomputing Institute (MSI) at the University of Minnesota for providing resources that contributed to the research results reported within this paper.

The authors declare no conflict of interest.

- [1] H. L. Liu, B. Zhang, T. Gao, X. Wu, F. Cui, and W. Xu, 3D chiral color prints for anti-counterfeiting, Nanoscale. 11, 5506 (2019).
- [2] A. Passaseo, M. Esposito, M. Cuscunà, and V. Tasco, Materials and 3D designs of helix nanostructures for chirality at optical frequencies, Adv. Opt. Mater. 5, 1601079 (2017).
- [3] S. Yoo and Q.-H. Park, Metamaterials and chiral sensing: A review of fundamentals and applications, Nanophotonics. **8**, 249–261 (2019).
- [4] A. Alvarez-Fernandez, C. Cummins, M. Saba, U. Steiner, G. Fleury, V. Ponsinet, and S. Guldin, Block copolymer directed metamaterials and metasurfaces for novel optical devices, Adv. Opt. Mater. 9, 2100175 (2021).
- [5] J. A. Dolan, R. Dehmel, A. Demetriadou, Y. Gu, U. Wiesner, T. D. Wilkinson, I. Gunkel, O. Hess, J. J. Baumberg, U. Steiner, M. Saba, and B. D. Wilts, Metasurfaces atop metamaterials: Surface morphology induces linear dichroism in gyroid optical metamaterials, Adv. Mater. 31, 1803478 (2019).
- [6] U. R. Gabinet and C. O. Osuji, Optical materials and metamaterials from nanostructured soft matter, Nano Res. 12, 2172 (2019).
- [7] C. Kilchoer, N. Abdollahi, J. A. Dolan, D. Abdelrahman, M. Saba, U. Wiesner, U. Steiner, I. Gunkel, and B. D. Wilts, Strong circular dichroism in single gyroid optical metamaterials, Adv. Opt. Mater. 8, 1902131 (2020).

- [8] S. S. Oh, A. Demetriadou, S. Wuestner, and O. Hess, On the origin of chirality in nanoplasmonic gyroid metamaterials, Adv. Mater. 25, 612 (2013).
- [9] S. S. Oh and O. Hess, Chiral metamaterials: Enhancement and control of optical activity and circular dichroism, Nano Converg. 2, 24 (2015).
- [10] M. Saba, M. Thiel, M. D. Turner, S. T. Hyde, M. Gu, K. Grosse-Brauckmann, D. N. Neshev, K. Mecke, and G. E. Schröder-Turk, Circular dichroism in biological photonic crystals and cubic chiral nets, Phys. Rev. Lett. 106, 103902 (2011)
- [11] M. Saba, B. D. Wilts, J. Hielscher, and G. E. Schröder-Turk, Absence of circular polarisation in reflections of butterfly wing scales with chiral gyroid structure, Materials Today Proceedings 1, 193 (2014).
- [12] J. A. Dolan, B. D. Wilts, S. Vignolini, J. J. Baumberg, U. Steiner, and T. D. Wilkinson, Optical properties of gyroid structured materials: From photonic crystals to metamaterials, Adv. Opt. Mater. 3, 12 (2015).
- [13] E. Goi, B. P. Cumming, and M. Gu, Gyroid "Srs" networks: Photonic materials beyond nature, Adv. Opt. Mater. 6, 1800485 (2018).
- [14] S. Vignolini, N. A. Yufa, P. S. Cunha, S. Guldin, I. Rushkin, M. Stefik, K. Hur, U. Wiesner, J. J. Baumberg, and U. Steiner, A 3D optical metamaterial made by self-assembly, Adv. Mater. 24, OP23 (2012).

- [15] B. M. Cote, W. R. Lenart, C. J. Ellison, and V. E. Ferry, Surface structure dependent circular dichroism in single and double gyroid metamaterials, Adv. Opt. Mater. 10, 2200363 (2022).
- [16] J. A. Dolan, K. Korzeb, R. Dehmel, K. C. Gödel, M. Stefik, U. Wiesner, T. D. Wilkinson, J. J. Baumberg, B. D. Wilts, U. Steiner, and I. Gunkel, Controlling self-assembly in gyroid terpolymer films by solvent vapor annealing, Small. 14, 1802401 (2018).
- [17] M. A. Chavis, D.-M. Smilgies, U. B. Wiesner, and C. K. Ober, Widely tunable morphologies in block copolymer thin films through solvent vapor annealing using mixtures of selective solvents, Adv. Funct. Mater. 25, 3057 (2015).
- [18] S. Jo, T. Jun, H. I. Jeon, S. Seo, H. Kim, S. Lee, and D. Y. Ryu, Optical reflection from unforbidden diffraction of block copolymer templated gyroid films, ACS Macro Lett. 10, 1609 (2021).
- [19] S. Jo, H. Park, T. Jun, K. Kim, H. Jung, S. Park, B. Lee, S. Lee, and D. Y. Ryu, Symmetry-breaking in double gyroid block copolymer films by non-affine distortion, Appl. Mater. Today. 23, 101006 (2021).
- [20] H.-Y. Hsueh, H.-Y. Chen, M.-S. She, C.-K. Chen, R.-M. Ho, S. Gwo, H. Hasegawa, and E. L. Thomas, Inorganic gyroid with exceptionally low refractive index from block copolymer templating, Nano Lett. 10, 4994 (2010).
- [21] F. Yu, Q. Zhang, R. P. Thedford, A. Singer, D.-M. Smilgies, M. O. Thompson, and U. B. Wiesner, Block copolymer selfassembly-directed and transient laser heating-enabled nanostructures toward phononic and photonic quantum materials, ACS Nano. 14, 11273 (2020).
- [22] X. Feng, C. J. Burke, M. Zhuo, H. Guo, K. Yang, A. Reddy, I. Prasad, R.-M. Ho, A. Avgeropoulos, G. M. Grason, and E. L. Thomas, Seeing mesoatomic distortions in soft-matter crystals of a double-gyroid block copolymer, Nature (London) 575, 175 (2019).

- [23] G. Fredrickson, *The Equilibrium Theory of Inhomogeneous Polymers* (Oxford University Press, Oxford, 2005).
- [24] J. Lequieu, T. Quah, K. T. Delaney, and G. H. Fredrickson, Complete photonic band gaps with nonfrustrated ABC bottlebrush block polymers, ACS Macro Lett. 9, 1074 (2020).
- [25] E. D. Palik, Handbook of Optical Constants of Solids (Academic Press, San Diego, 1998).
- [26] A. Arora, J. Qin, D. C. Morse, K. T. Delaney, G. H. Fredrickson, F. S. Bates, and K. D. Dorfman, Broadly accessible selfconsistent field theory for block polymer materials discovery, Macromolecules. 49, 4675 (2016).
- [27] A. Arora, D. C. Morse, F. S. Bates, and K. D. Dorfman, Accelerating self-consistent field theory of block polymers in a variable unit cell, J. Chem. Phys. 146, 244902 (2017).
- [28] G. K. Cheong, A. Chawla, D. C. Morse, and K. D. Dorfman, Open-source code for self-consistent field theory calculations of block polymer phase behavior on graphics processing units, Eur. Phys. J. E. **43**, 15 (2020).
- [29] S.-M. Yang, J. Oh, B. R. Magruder, H. J. Kim, K. D. Dorfman, M. K. Mahanthappa, and C. J. Ellison, Surface relief terraces in double-gyroid-forming polystyrene-block-polylactide thin films, Phys. Rev. Mater. 7, 125601 (2023).
- [30] B. R. Magruder, D. C. Morse, C. J. Ellison, and K. D. Dorfman, Boundary frustration in double-gyroid thin films, ACS Macro Lett. 13, 382 (2024).
- [31] See Supplemental Material at http://link.aps.org/supplemental/ 10.1103/PhysRevMaterials.8.115201 for additional simulation results including for the (211) orientation, additional compression of double gyroid films, compression of double gyroid films using Poisson's ratio, stretching of double gyroid files, and additional cumulative circular dichroism depth profiles.
- [32] https://10.13020/rka8-vd05
- [33] https://github.com/dmorse/pscfpp